The Proton EDM Ring Lattice and UAL/ETEAPOT Simulation Software

Richard Talman

March 14, 2011, BNL Review

1 UAL/ETEAPOT Simulation Software

- To introduce the most important recent advance in our understanding, I will discuss simulation first, but only very briefly. (See accompanying report *Development of the UAL/ETEAPOT Code for the Proton EDM Experiment,* by Malitsky, John Talman, and RT.) Further ETEAPOT details will be reserved for the end of the talk.
- Show UAL/ETEAPOT proton EDM ring tracking results which indicate what seems to be the most important difference between electric and magnetic rings
- *Horizontal oscillations in electric ring fail to respect the fast-slow, Courant-Snyder, betatron-synchrotron paradigm*
- Strong coupling between longitudinal and horizontal oscillations i.e. synchrobetatron coupling
- Fast mixing between horizontal and longitudinal amplitudes may permit much lower RF frequency, and longer bunches, than would otherwise be required
- FFT analysis of the tracking results also provide independent confirmation of electric transfer matrix formalism.

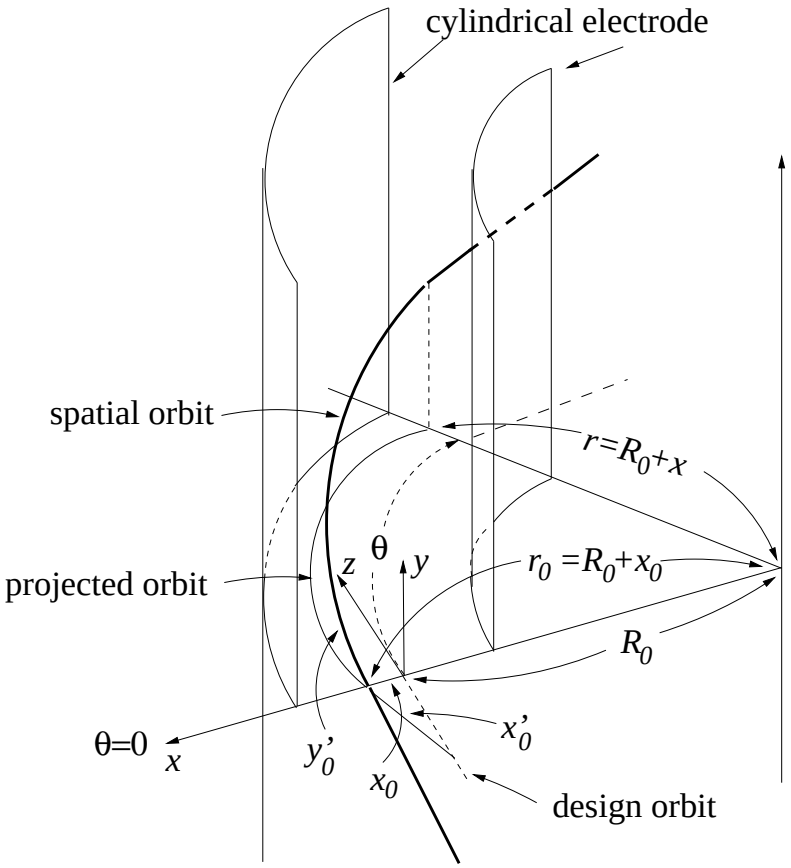

Figure 1: The bold curve shows a proton orbit passing through a curved-planar cylindrical electrostatic bending element. The electrode spacing is g and the design orbit is centered between the electrodes.

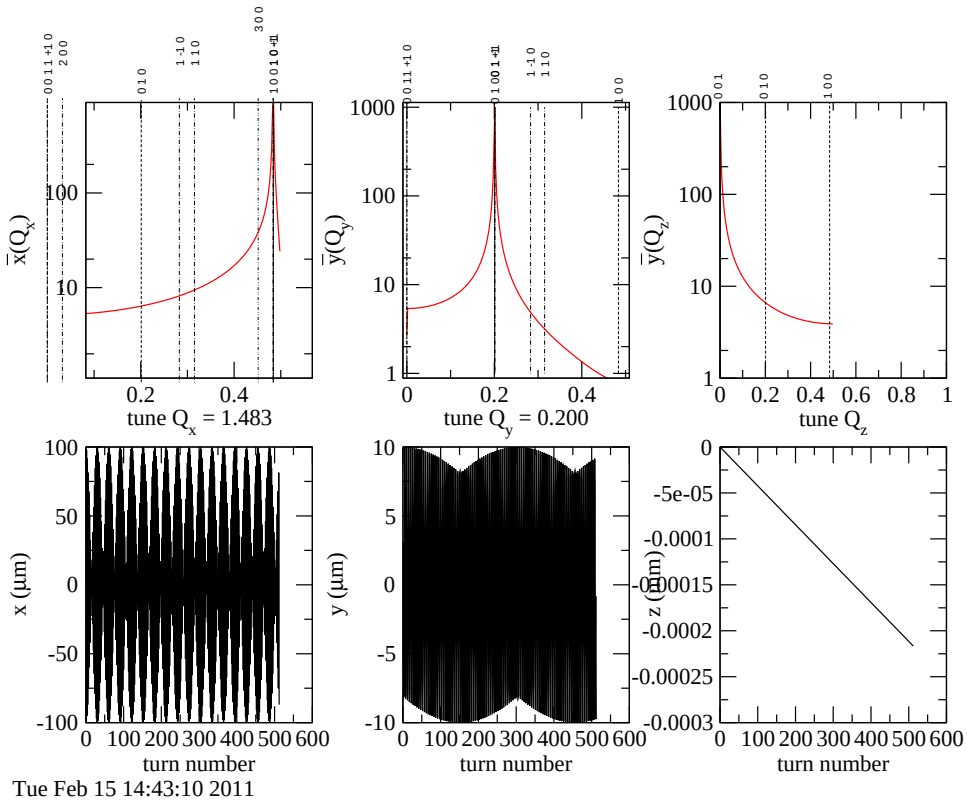

Figure 2: Tracking results for simultaneous vertical and horizontal motion of one particle in an idealized "first test" ring.

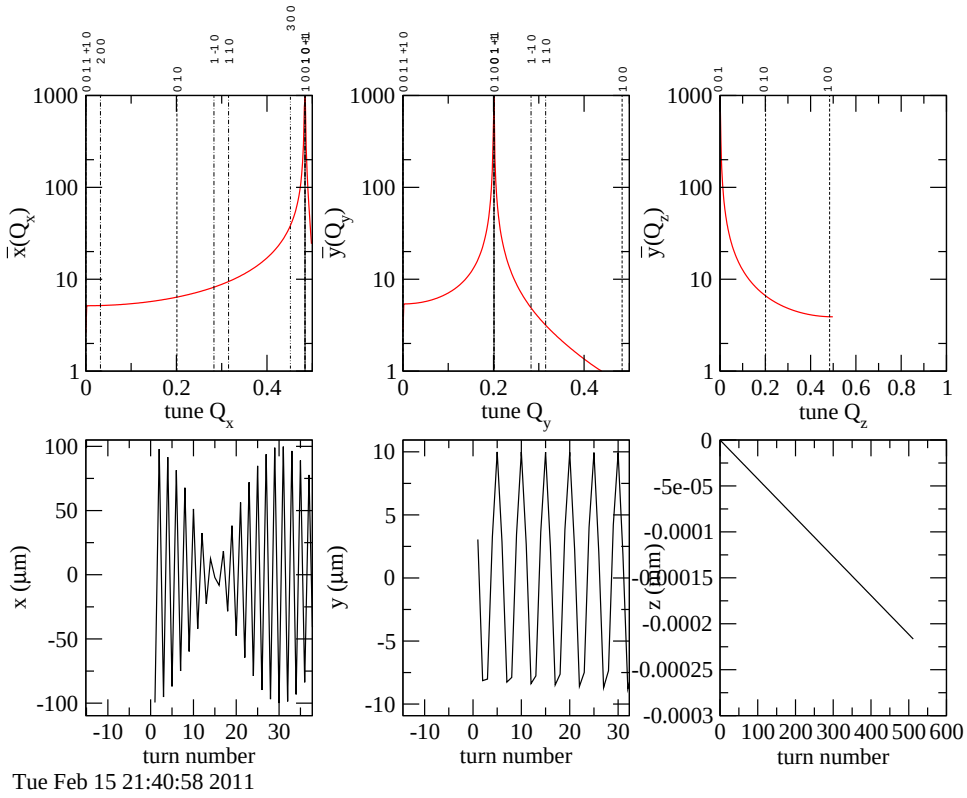

Figure 3: The beat pattern indicates sloshing back and forth between horizontal and longidinal amplitudes. Vertical oscillations are only affected weakly.

2 Proton EDM Ring Lattice Optics

After showing the table of contents for the accompanying report, the rest of the talk consists mainly of showing and explaining figures from that report.

Contents

Abstract.

- The ring is, first, an accelerator and second (but foremost) a physics experiment. This report discusses the optimization of the ring for its experimental purpose and to demonstrate its adequacy as an accelerator that can store enough oriented protons for long enough.
- The more delicate issues governing the experiment itself are discussed by others.
- As well as being analytically cantankerous (infinite dispersion, for example), the $1/r$ electric field dependence, that was initially taken to be nominal, imposes serious injection difficulties and leads to unacceptably small spin coherence time (SCT). Electric field variation closer to independent of r is investigated and found to be essential. Saddle-shaped electrodes (inward curvature horizontally, outward curvature vertically) are needed to produce this field variation.
- To meet the $\partial^2 T_{\mathrm{rev.}}/\partial\gamma^2 = 0$, SCT, revolution period constraint, the total straight section length $D_{\mathrm{tot.}}$ has to be minimized, since the constraint can just barely be satisfied with realistic lattice elements. This requires careful budgeting of the lengths and numbers of all lattice elements.
- Together, these considerations largely dictate the lattice design.

2.1 Previous Electric Rings

- The proposed electrostatic storage ring for the proton EDM experiment will be more than ten times larger than any previous electrostatic ring. In spite of this, its betatron tunes will be less than any of these earlier rings. Because of their strong focusing, beam dynamics in these predecessor rings scarcely distinguished between electric and magnetic dynamics. In fact the AGS-Analog ring built at BNL was regarded as a prototype for the magnetic AGS.
- The main challenges for the EDM ring will be precision vertical beam position monitoring and achieving adequately long spin coherence time (SCT). Both of these favor extremely low tunes. Low tune values amplify the differences between magnetic and electric focusing, differences resulting from the variation of particle speed in electric, but not magnetic, fields.

Table 1: Brief chronology of EDM lattice development

index	lattice type	shape	date	novel feature	feature survival	comment
(i)		ra.tr.	2008	deuteron	x	ceded to COSY
				carbon polarimetry	$\surd$	
(ii)	SF	ra.tr.	12/7/09	proton	$\surd$	
				magic momentum	$\surd$	spin tracks momentum
(iii)	CDSF	ra.tr.	4/25/10	electric focusing	$\surd$	
				toroidal electrodes	x$\rightarrow \surd$	high focusing strength not needed
				combined function	x$\rightarrow \surd$	
(iv)	SF	ra.tr.	5/20/10	latt.sp. = bunch sp.	$\surd \rightarrow$ x	for resonant BPM's
				p-p polarimetry, low β IP	x$\rightarrow \surd$?	p-p colliding beam rate too low, (but internal H target?)
				compensate spin decoher.	$\surd$	
				"managed" dispersion	$\surd$	but *not* zero dispersion
(v)	SF	circle	8/15/10	high multiperiodicity	$\surd$	no benefit from race track and
				realistic straight secs.	$\surd$	BPM's need many longish straights
(vi)	SF	ra.tr.	8/15/10	$Q_y << 1$ for y meas. prec.	$\surd$	
				$Q_y << 1$ (for insensitivity	x	$\gamma_y >> 1$ defeats $\beta_y >> 1$ which
				to vertical betatron osc.)		*demands* combined function
(vii)	wCFSD*	circle	8/15/10	*weak* comb. func. focus.	$\surd$	phony magnetic orbitry no longer
				long BPM's	x	tolerable for $Q_{x,y} \sim 1$ elec. latt.
(viii)			1/1/11	$Q_y << 1$, SCT y-insensitiv.	$\surd$	$\langle \alpha_y \rangle << 1$
(ix)	wCFSDrtr	ra.tr.	1/6/11	BPM, etc. lengths minimized	$\surd$	to increase SCT
				electron cooled injection	$\surd$ x	unjustified for injection phase space matching
				saddle-shaped electrodes	$\surd$	$\partial^2 T/\partial \gamma^2 \approx 0$, to increase SCT
				linac/cyclotron RF	$\surd$	
(x)	wCFSDrtr	ra.tr.	1/16/11	SCT compensation	$\surd$	three sextupole family compensation
	"baseline"			improved lattice symmetry	$\surd$	
	`pEDM.rtr1`			integral BPM, quad,sext module	$\surd$	BPM's 10 $\rightarrow$ 16
			2/11/11	dedicated magnetometer modules	$\surd$	magnetic shielded squids

* "wCFSD" stands for "(weak) Combined function Focusing, Separate function Defocusing."

Table 2: Lattice parameters for successive lattice iterations. Variant (x) has become the "baseline" design.

index	lattice type	shape	circum. m	cell len. m	BPM slot len. (m)	arcs, cells/arc	Q_x	Q_y	$\int \gamma_x ds$	$\int \gamma_y ds$	$\beta_x^{\max}$ m	$\beta_y^{\max}$ m	$D^{\max}$ m
(i)		ra.tr.	83	10.4	small	2 x 4	4.25	3.80			11.7	13.3	3.0
(ii)	SF	ra.tr.	250	6.2	0.15	2 x 16	7.9	9.8			10.3	10.3	1.28
(iii)	CDSF	ra.tr.	253	5.2	0.18	2 x 20	12.6	8.6			8	10	0.7
(iv)	SF	ra.tr.	420	25	0.18	2 x 8	12.6	8.6			8	10	6
(v)	SF	circle	251	15.7	2.0	20	2.7	0.29	**28.5**	**80.4**	21	190	
(vi)	SF	ra.tr.	450	15.7	2.0	2 x 10	4.4	0.21			32	450	
(vii)	CFSD	circle	271	8.48	2.0	32	1.53	0.20	**9.6**	**1.9**	28	218	
(viii)	CFSD	circle	268.496	6.712	2.0	20	1.516	0.201	**9.532**	**1.261**	28.3	213	18.6
(ix)	CFSD	ra.tr.	259.327	32.4	0.3	2 x 4	1.346	0.202	**8.857**	**3.747**	33.1	231	23.6
(x)	CFSD	ra.tr.	263.427	32.316	0.45*	2 x h,3,h*	1.304	0.202	∼**8.9**	∼**3.7**	27.9	246	25.3

* BPM,quad,sext merged in single slot, h,3,h indicates 1/2 cell, 3 full cells, 1/2 cell

3 Minimal, Weak Focusing, Racetrack CFSD Lattice

- "CFSD" in the section title stands for "Combined function Focusing, Separate function Defocusing". One cell of this lattice is shown in Fig. 5. The full ring is shown in Fig. 4.
- More detailed element parameters are in the MAD listing `E_pEDM-rtr1.mad` in Appendix 9. This MAD file cannot be processed directly by MAD-like programs, because such programs implicitly assume that elements are magnetic and, furthermore, MADX does not support the index m, power law field index.
- This file has tentative A, B, C family sextupole strengths included.
- The arc length rationing "budget" is shown in Table 4.
- Focusing, steering, sextupoles, and BPM's share the same intrumentation units.
- Six units are primarily for magnetometers. Eight are primarily for vertical focusing and vertical tune modulation.

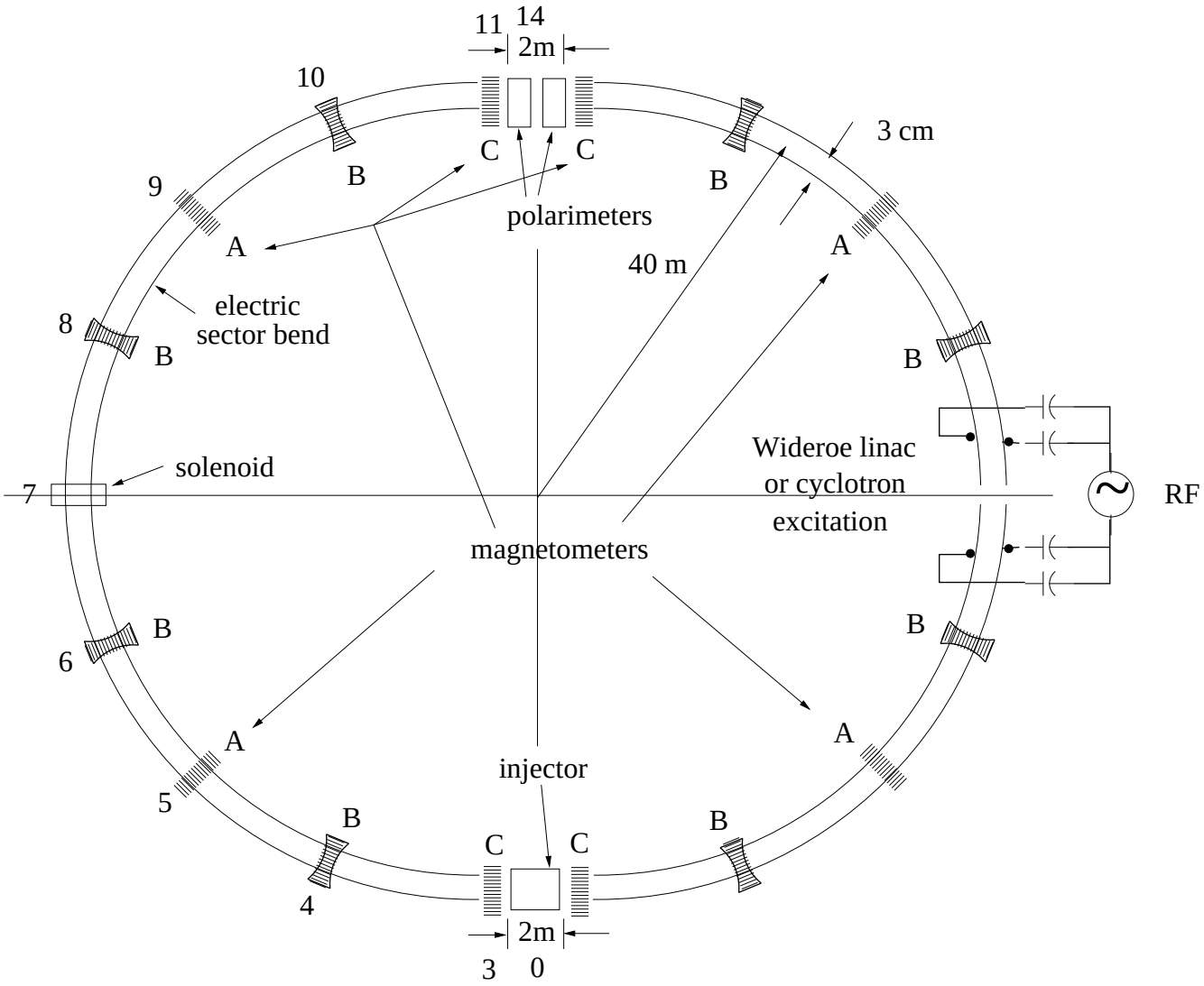

Figure 4: Identification of sextupole family locations for "baseline" design. All shaded sections contain the same quad, sext, BPM, integrated package; those with quads symbols superimposed (label B) provide the dominant vertical focusing.

Table 3: Integrated optical strengths (preliminary) of quadrupoles and sextupoles in packages A, B, and C. Sextupole strengths still need to be modified by the factor η_D which depends on the definition of "dispersion".

package	β_x m	β_y m	q m^{-1}	S m^{-2}	$(\lvert S\rvert\beta_x)^{-1}$ m	$(\lvert S\rvert\beta_y)^{-1}$ m
A	26.5	197.8	0	$0.00465/\eta_D$	$8.1\eta_D$	$1.1\eta_D$
B	22.4	231.0	0.02366	$-0.00253/\eta_D$	$17.0\eta_D$	$1.7\eta_D$
C	26.5	180.2	-0.002	$-0.00088/\eta_D$	$43\eta_D$	$6.3\eta_D$

Table 4: Arc length budget for $R_0 = 40\,\mathrm{m}$. The maximum allowable total straight section length has been found to be 11.6 m. The maximum can be increased (more or less proportionally) by allowing $R_0 > 40\,\mathrm{m}$.

element type	number of elements	length per element	total length	comment
RF	0		0.0	Wideröe linac/"cyclotron"
solenoid	1	0.3	0.3	
quad, sext, BPM	16	0.45	7.2	integrated package
polarimeter	2	1.0	2.0	
injection	1	2.0	2.0	uncooled, correlated, horz.
total			11.5	

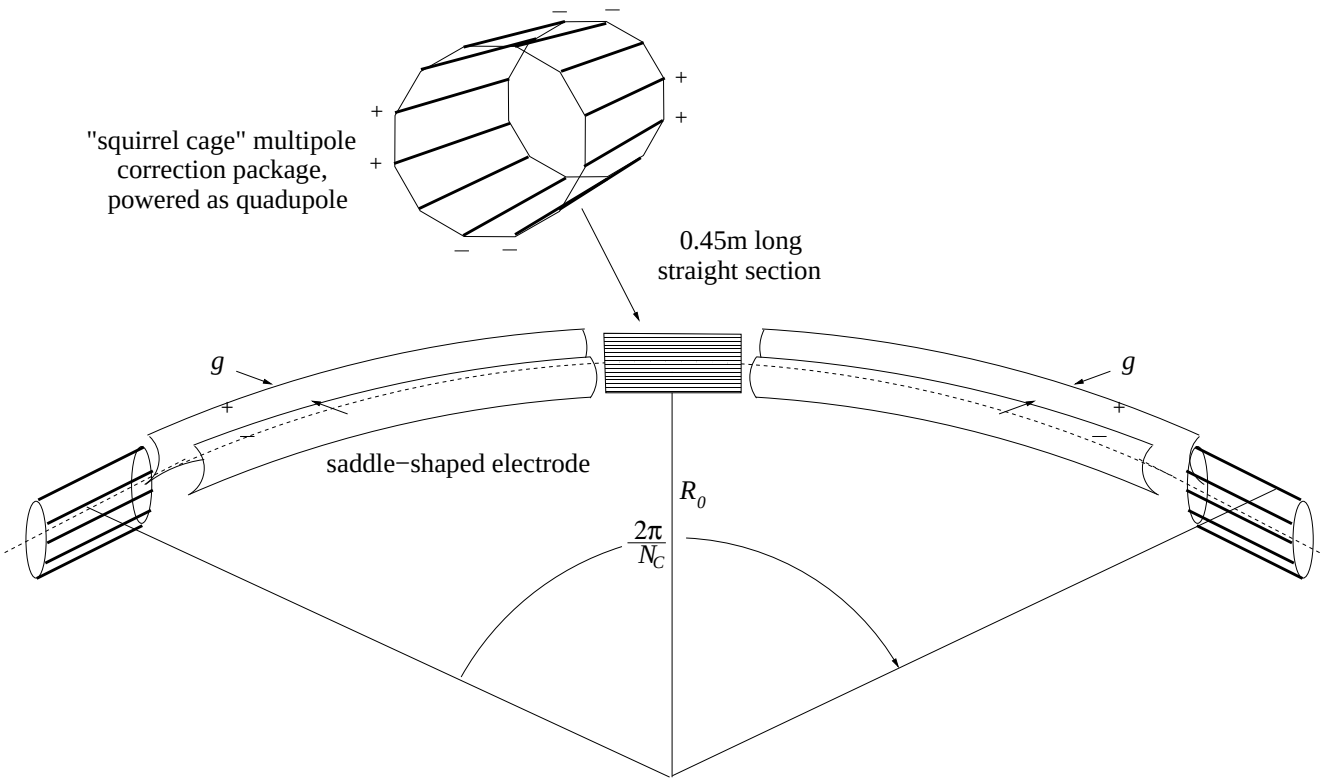

Figure 5: Sketch of one cell of baseline `pEDM-rtr1` EDM lattice.

Table 5: Horizontal optical functions for one half of wCFSD lattice. $Q_x = 1.304$.

label	position	β_x	α_x	γ_x	D	sext.
	m	m		1/m	m	family
0	0.000	26.452	-0.3308	0.04194	25.292	origin
1	1.000	26.477	-0.3557	0.04254	25.292	
2	1.150	26.481	-0.3329	0.04194	25.290	
3	1.225	26.482	-0.3348	0.04199	25.289	C
4	17.383	21.333	-0.3311	0.05201	22.254	B
5	33.541	26.507	-0.3536	0.04244	23.582	A
6	49.699	22.404	-0.3535	0.05021	20.972	B
7	65.857	27.806	-0.3308	0.03989	22.836	slnd
8	82.015	22.404	-0.3082	0.04887	20.972	B
9	98.173	26.507	-0.3080	0.04130	23.581	A
10	114.331	21.333	-0.3305	0.05199	22.252	B
11	130.489	26.482	-0.3268	0.04179	25.288	C
12	130.564	26.481	-0.3287	0.04184	25.290	
13	130.714	26.477	-0.3059	0.04130	25.291	
14	131.714	26.452	-0.3308	0.04194	25.291	mid pt.

Table 6: Vertical optical functions for one half of wCFSD lattice. $Q_y = 0.202$.

label	position	β_y	α_y	γ_y	sext.
	m	m		1/m	family
0	0.000	180.129	0.0000	0.005552	origin
1	1.000	180.135	-0.0056	0.005552	
2	1.150	180.164	-0.1865	0.005744	
3	1.225	180.192	-0.1870	0.005744	C
4	17.383	231.034	-0.2940	0.004702	B
5	33.540	197.796	-0.2052	0.005269	A
6	49.698	246.003	-0.1054	0.004110	B
7	65.856	204.127	0.0000	0.004899	slnd
8	82.014	246.003	0.1054	0.004110	B
9	98.172	197.796	0.2052	0.005269	A
10	114.330	231.034	0.2940	0.004702	B
11	130.488	180.192	0.1870	0.005744	C
12	130.563	180.164	0.1865	0.005744	
13	130.713	180.135	0.0056	0.005552	
14	131.713	180.129	0.0000	0.005552	mid pt

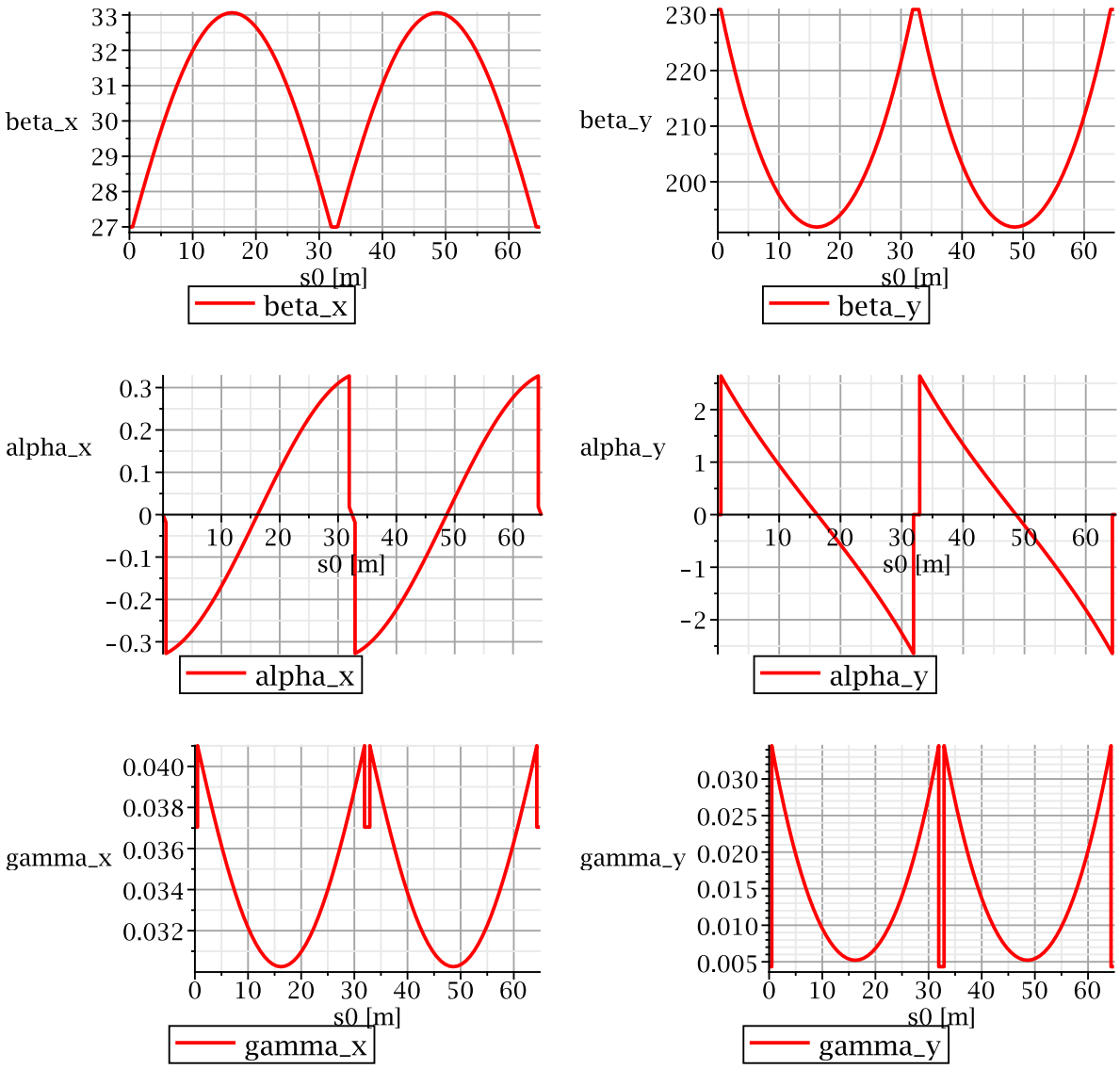

Figure 6: Plots of lattice functions for two cells of baseline lattice. Betatron oscillation induced spin decoherence is proportional to average values of γ_x and γ_y.

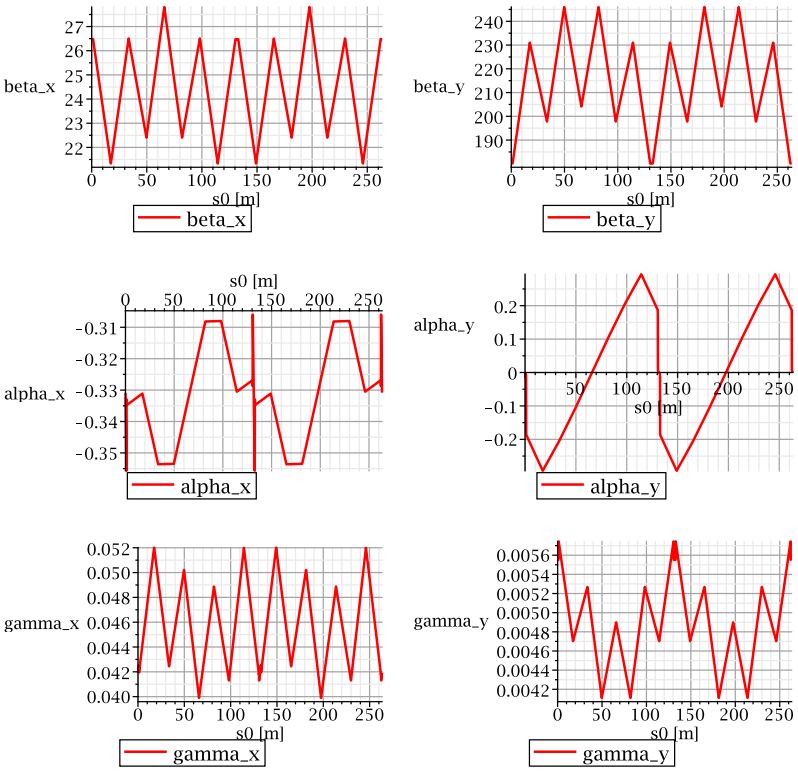

Figure 7: Plots of lattice functions for version (x) racetrack-shaped lattice.

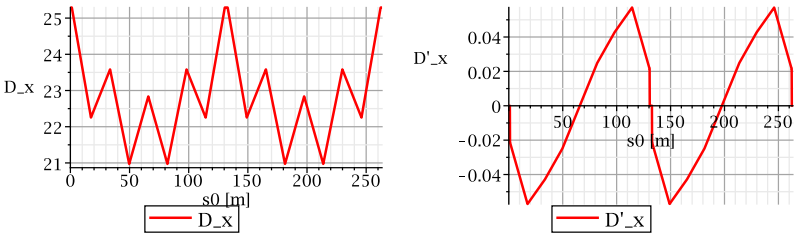

Figure 8: Dispersion $D_x(s_0)$ and dispersion slope $D'_x(s_0)$, functions of longitudinal position s_0. This dispersion function is referenced to rigidity offset Δ, *outside bend elements*.

4 Magnitometer and Vertical Focusing Instrumentation Packages

- An initial lattice design had a single multipurpose beam position, beam corrector unit, applicable at all 16 intrumentation straight sections.
- It was found, however, that squid magnetometer units will need the lion share of their own straight sections.
- By far the greatest multipole strength is required for the eight B locations which provide vertical focusing. The vertical tune modulation is driven at these same B locations.
- Furthermore, for signal processing reasons, modulation and magnetometers cannot be in the same lattice straight sections.
- The forced compromise, therefore, was to introduce dedicated magnetometer and dedicated modulated vertical quad units.
- All B locations have quad units, all A and C (except the two C locations adjacent to the injection straight) have magnetometer units.

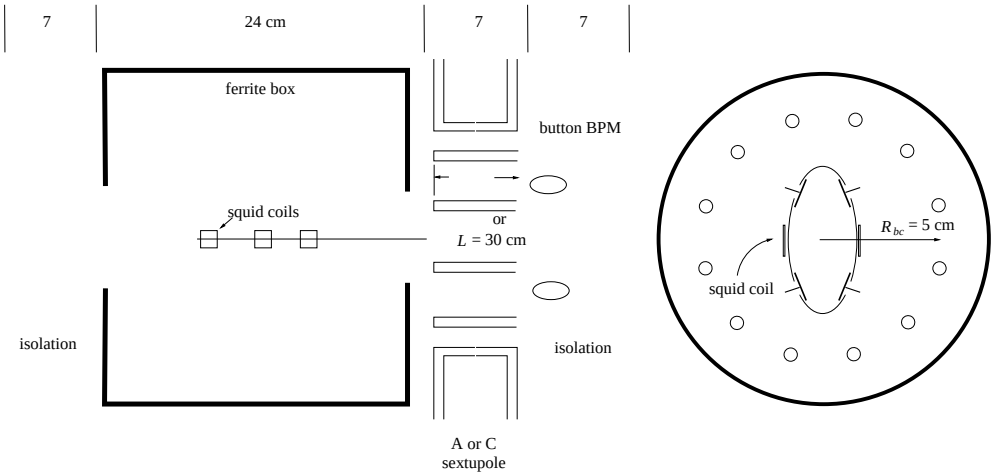

Figure 9: Dedicated magnetometer packages at A and C locations.

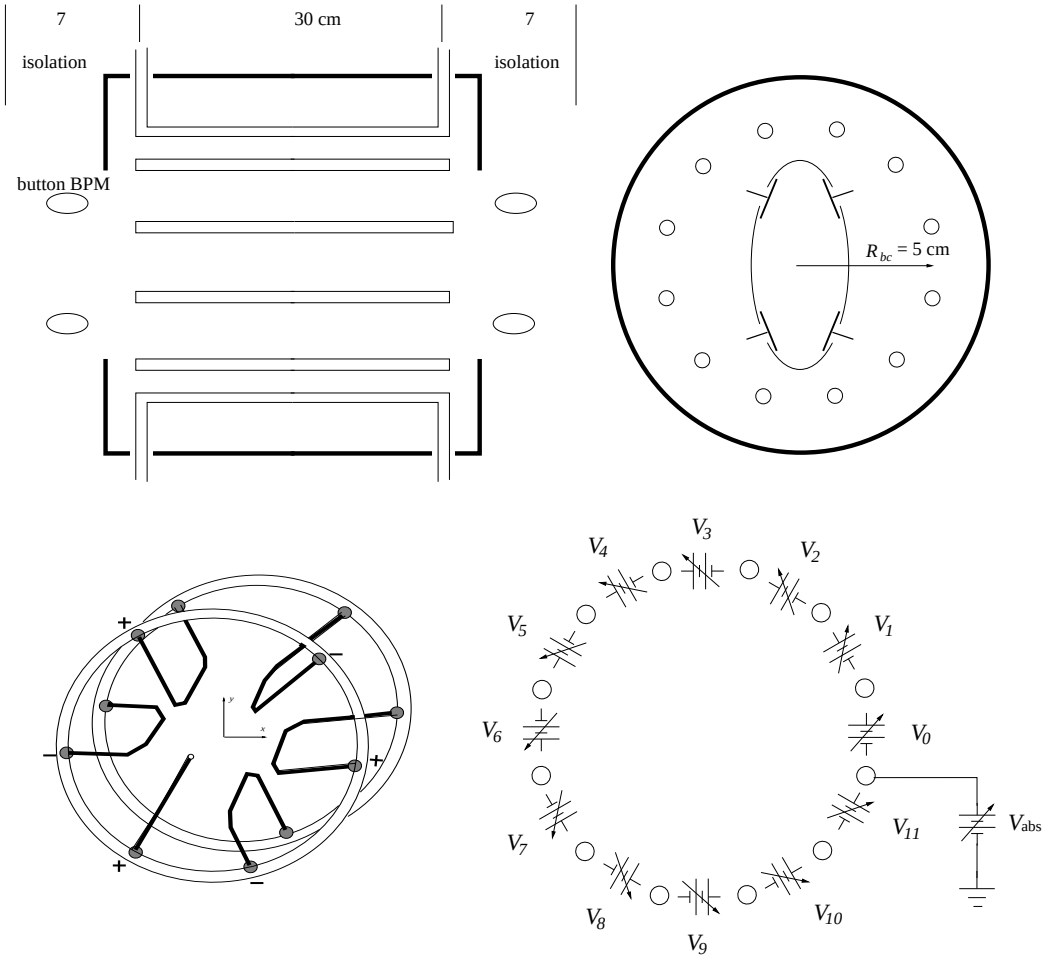

Figure 10: Multipurpose, squirrel cage, quadrupole, sextupole, steering correction, and button BPM at B locations.

The dominant requirement of the squirrel cage package is to provide B-family vertical focusing quadrupoles with (from Table 3) strength $q_y = 0.024\,\mathrm{m}^{-1}$. The required potential energy coefficient, for symmetric operation, is therefore

$$V^C_{2,\mathrm{symm.}} = q_y \beta_0 (p_0 c/e)\,\frac{R^2_{\mathrm{sq}}}{2L_{\mathrm{sq}}} \stackrel{\text{e.g.}}{=} 0.024 \times 0.6 \times 0.7 \times 10^9\,\frac{0.05^2}{0.60} = 42 \times 10^3\,\mathrm{V}. \tag{1}$$

For quadrupole powering the maximum voltage drop between adjacent electrodes is equal to the maximum absolute voltage. An approximately optimal geometry has the electrode rod diameters equal to the vacuum gap length between adjacent electrode surfaces. Using the same prescription as has been used to establish the maximum bending electric field (see Bill Morse presentation), the maximum interelectrode voltage is $45 \times 10^3\,\mathrm{V}$.

4.1 Application of Universal Focusing Unit for Vertical Tune Modulation

ΔQ_y (equal, say, to 0.1) due to a change Δq_y, at a position in the lattice where the beta function is β_y;

$$\Delta Q_y = N_B \frac{\Delta q_y \beta_y}{4\pi}. \tag{2}$$

A factor $N_b = 8$, the number of B-type quadrupoles has been included.

$$\Delta q_y = \Delta Q_y \, \frac{4\pi}{N_B \beta_y} \stackrel{\text{e.g.}}{=} 0.1 \, \frac{4\pi}{8 \times 231} = 0.69 \times 10^{-3}. \tag{3}$$

Expressed as a ratio to the absolute value of the B-type quadrupoles this is

$$\frac{\Delta q_y}{q_y} = \frac{0.69 \times 10^{-3}}{0.024} = 0.028. \tag{4}$$

4.2 Large Energy-Offset Closed Orbits

- Fig. 11, shows the dependence of $T_{\text{rev.}}$ on γ^O, for the now-obsolete lattice version (*viii*), over a vastly greater range than is actually needed.
- The (damaging to SCT) upward curvature is due to the excessively long straight sections in lattice design (*viii*).

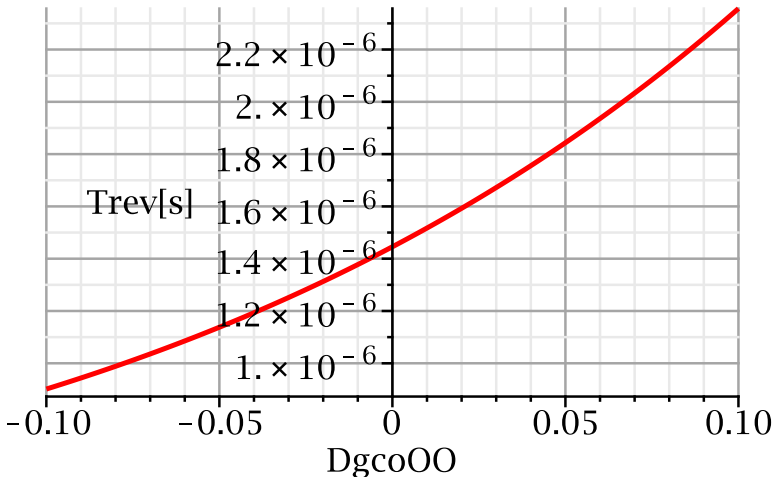

Figure 11: Revolution period $T_{\text{rev.}}$ as a function of $\Delta\gamma^O$ (which is labelled "DgcoOO" in the plot) for the now-obsolete lattice design (*viii*). (To make the curvature visible) this plot, calculated from exact equations, extends over a vastly greater range than previous plots. Its analytical form is $T_{\text{rev.}} = 1.49672 + 1.734\,\Delta\gamma^O + 4.86\,\Delta\gamma^{O\,2}\,\mu$s.

4.3 Tailoring the Field Index to Improve Spin Coherence

- The field index m, which is 1 for inverse square law, 0 for logarithmic potential, is used in this section.
- The field index m can be adjusted using toroidal or saddle-shaped electrodes. It is possible to reduce spin decoherence by synchronized adjustment of m and the accumulated length $D_{\text{tot.}}$ of all straight sections.
- The closed orbit of an off-energy particle in bends is a circle, with radius r given by

$$r^m = R_0^m \frac{eE_0R_0}{m_pc^2} \frac{\gamma^I}{\gamma^{I2}-1} = R_0^m \frac{\gamma_0^2-1}{\gamma_0} \frac{\gamma^I}{\gamma^{I2}-1} \tag{5}$$

- The superscripts I have been attached to kinematic quantities to indicate that they are being evaluated "inside" the bending element. The electric potential at radius r is given by,

$$V(r) = -\frac{E_0R_0}{m}\left(\frac{R_0^m}{r^m}-1\right), \tag{6}$$

so the mechanical energy outside $m_pc^2\gamma^O$ is related to the mechanical energy inside $m_pc^2\gamma^I$ by

$$\gamma^O = \gamma^I - \frac{1}{m}\frac{eE_0R_0}{m_pc^2}\left(\frac{R_0^m}{r^m}-1\right). \tag{7}$$

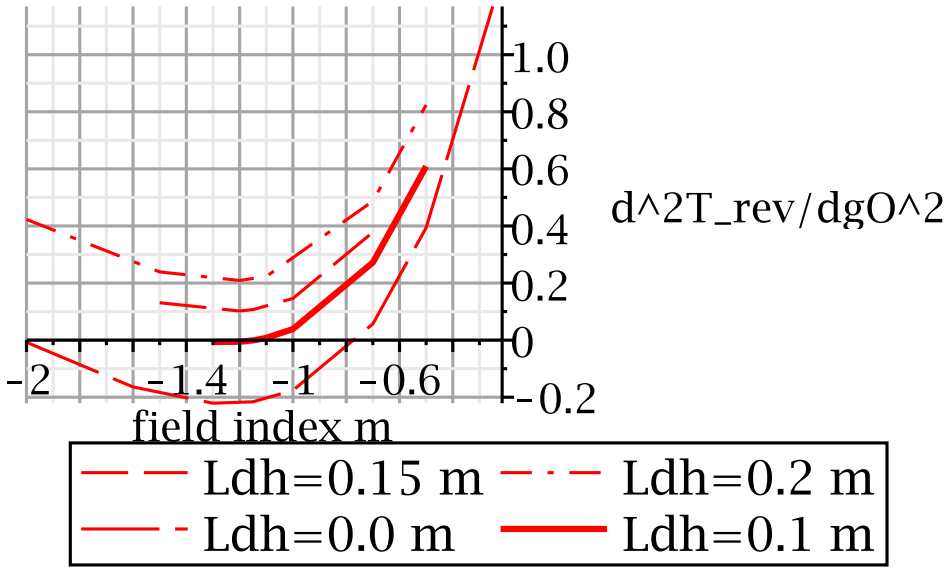

Figure 12: Dependence of the quadratic coefficient $d^2T_{\mathrm{rev.}}/d\gamma^{O\,2}$ as a function of field index m for various values of the straight section half length "ldh" for lattice version (*viii*). In this version there were 40 straight sections, each 2 m long. The bold line shows the largest drift length consistent with vanishing quadratic coefficient.

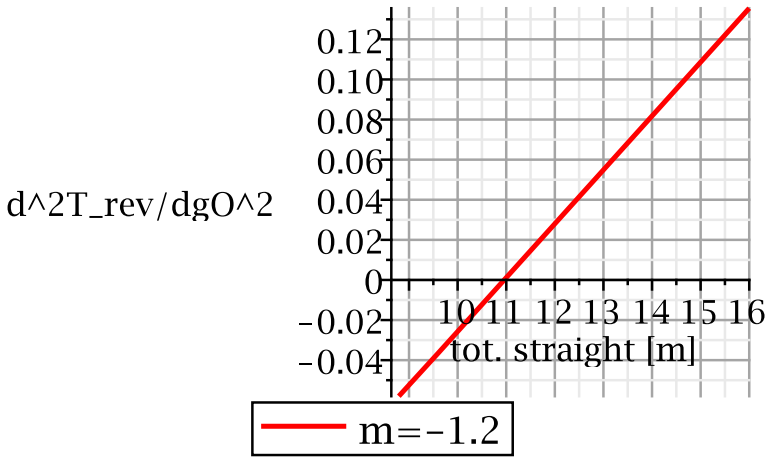

Figure 13: For lattice version (ix), and presumably also version (x), the dependence of the quadratic coefficient $d^2T_{\text{rev.}}/d\gamma^{O\,2}$, for field index $m = -1.2$, as a function of total straight straight section length $D_{\text{tot.}}$. The zero crossing fixes $D_{\text{tot.}} = 11.0\,\text{m}$ for $m = -1.2$.

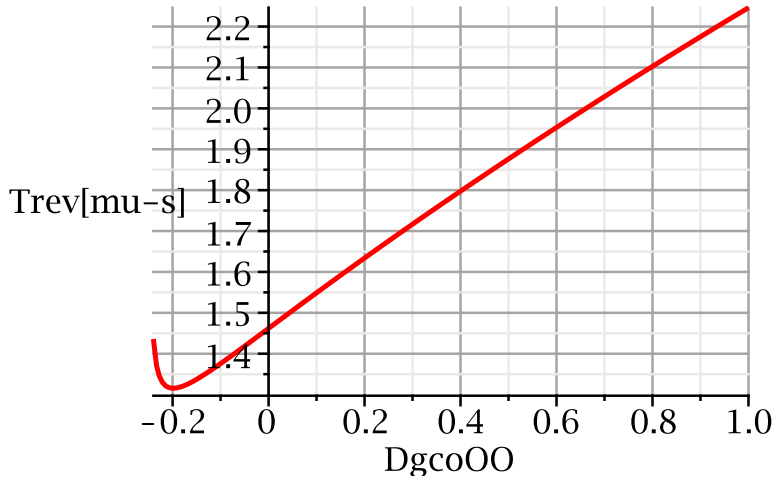

Figure 14: The dependence of $T_{\text{rev.}}$ on $\Delta\gamma^O$ over a range of $\Delta\gamma^O$ that is huge compared to the actual range needed for the experiment. The Taylor series expansion is $T_{\text{rev.}} = 1.46211 + 0.874\,\Delta\gamma^O + 0.0000673\,\Delta\gamma^{O^2} + \ldots\,\mu$s.

To correlate with standard formulas one can use the so-called "slip factor" η_{rf},

$$\eta_{\text{rf}} = \frac{dT_{\text{rev.}}/d\gamma^O}{T_0}\,\beta_0\gamma_0 = \frac{0.874}{1.462} \times 0.5984 \times 1.248 = 0.446. \qquad (8)$$

5 Injection Specification

5.1 Energy-Referenced Dispersion $D_{\mathcal{E}}$

The off-energy closed orbit is plotted in Fig. 15. This yields $D_{\mathcal{E}} = 0.046/0.001 = 46\,\mathrm{m}$. Fitting to the average value shown in Fig. 8, we obtain

$$\frac{D_{\mathcal{E}}}{D_x} \approx \frac{51}{22.8} = 2.24. \tag{9}$$

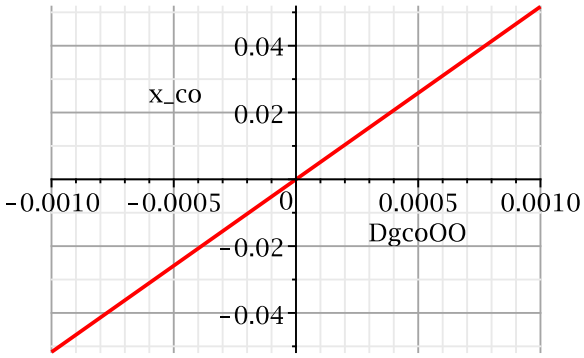

Figure 15: Dependence on $\Delta\gamma^O$ of the off-energy closed orbit $x_{\mathrm{co}.}$. Its slope gives the energy-referenced dispersion function $D_{\mathcal{E}}(\Delta\gamma^O)$.

5.2 Injection Hardware

- The requirement of using only electric fields for the EDM experiment has the important disadvantage that achievable electric deflection is way weaker than achievable magnetic deflection.
- There is, however, one important advantage of electric deflection—the deflection hardware has negligible "inertia". In the electric case it is the capacity of sector bend elements that constitute the inertia. The capacity is a (very small)

$$C_{2\pi/16} = 10^{-11}\,\frac{15 \times 0.2}{0.03} = 1.1\,\mathrm{nF}. \tag{10}$$

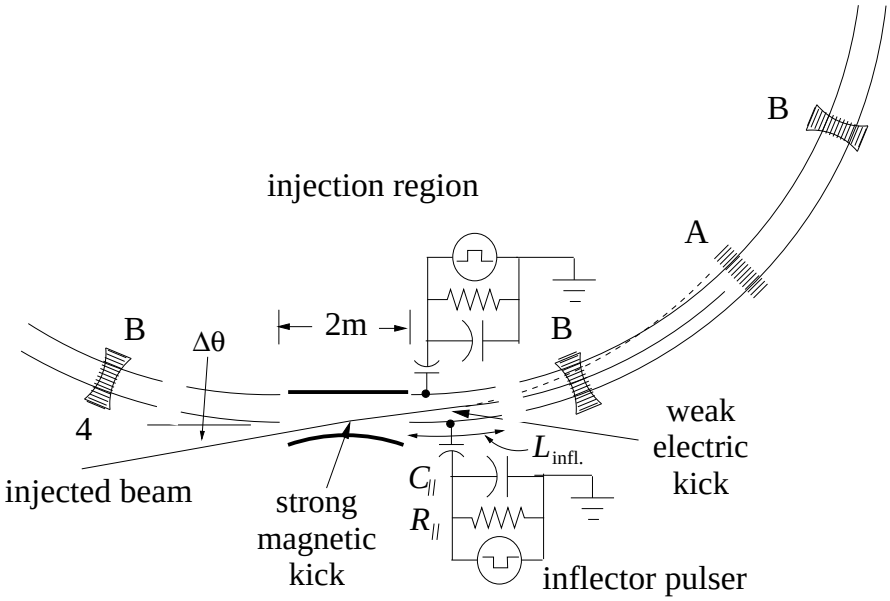

Figure 16: Crude schematic illustrating "two bump" injection into the ring. A strong magnetic kick removes most of the original angular divergence $\Delta\theta$. A weak electric bump applied by the inflector pulsers to a short initial bend section steers the beam onto the design orbit, such that no protons follow the broken line to be lost on the inner electrode.

- A cartoon of a possible injection scheme is shown in Figure 16. Just before injection the injected beam inclination is $\Delta\theta$. The detailed design depends on the value of $\Delta\theta$. The figure illustrates a two bump scheme which employs a magnetic deflector.
- Philip Pile showed that an earlier proposed scheme would have been unsatisfactory since most of the beam would follow the dashed line shown in the figure and would wipe out on the inner electrode.
- Injection into the proton EDM ring shares many requirements with injection into the muon G-2 experiment ring, the most important of which being that there be no magnetic materials. Magnetic deflection

therefore requires air core coils. Another concern for G-2, eddy current fields, on millisecond time scales, are unimportant for the EDM experiment. Required parameters for the EDM experiment are compared with those for the muon G-2 inflector in Table 7.

Table 7: Parameters of air core magnetic inflector parameters for the muon G-2 and what would be required for magnetic inflection proton EDM ring.

parameter	unit	muon G-2	proton EDM	"ease" factor
momentum	GeV/c	3.1	0.7	4.4
deflection angle	mrad	10	25	0.4
length	m	5.1	1.8	0.35
width	cm	10	6	1.7
height	cm	10	10	1.0
FWHM	ns	240	240	1.0
"ease" product				1.05

6 "Cyclotron" Operation

The design revolution period of the ring is $T_0 = 1.4621\,\mu$s, which corresponds to a revolution frequency $f_0 = 0.6839\,$MHz. The design RF frequency is

$$f_{RF} = hf_0 = 101 \times 0.6839 = 69.1\,\text{MHz}, \tag{11}$$

where harmonic number $h = 101$ has been assumed.

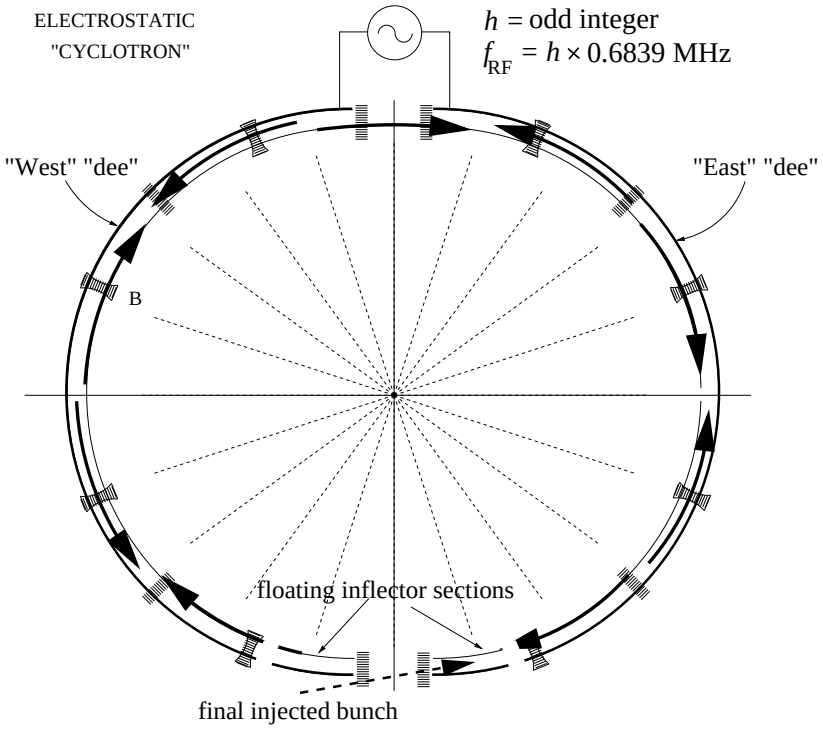

Figure 17: The proton EDM ring implemented as an electrostatic cyclotron. To simplify this figure the bunch lengths are impractically long. There are nine buckets already filled and the tenth bucket is in the process of being filled. For currently anticipated EDM parameters a much higher harmonic number, such as $h = 101$, is required in order to reduce the angular range of spin slewing relative to momentum. These buckets would be too closely spaced to fill every bucket in the way shown. Direct injection into every fifth bucket could, perhaps, be achieved.

6.0.1 Synchrotron Tune, Q_s

Because there are two gaps, the total RF voltage $V_{\rm RF}$ is $2V$, where V is the voltage between the two dees. The synchrotron tune is given by

$$\begin{aligned} Q_s &= \sqrt{\frac{h\eta_{\rm rf}}{2\pi\beta_0^2\gamma_0}}\sqrt{\frac{V_{\rm rf}}{m_pc^2/e}} \\ &= \sqrt{\frac{0.267\times 2\times 101}{2\pi 0.598^2\times 1.248\times 0.938\times 10^9}}\sqrt{V[\text{volts}]} \\ &= 1.432\times 10^{-4}\sqrt{V[\text{volts}]} \end{aligned} \tag{12}$$

To obtain $Q_s = 0.01$ requires $V = 4900\,\text{V}$.

6.0.2 Maximum Deviation, $\alpha_{\rm max.}$, From Proton Direction

Because of its deviation $\Delta\gamma$ from the magic factor γ_0, the proton spin orientation angle α precesses away from the proton momentum direction. However synchrotron oscillation stability prevents the secular growth of this deviation. The synchrotron tune has to be high enough to hold the maximum deviation less than some specified maximum tolerance, say $\alpha_{\rm max.} = 0.1\pi$. (Substantially greater deviation than this would begin to reduce the "signal" which is the up/down tipping of the proton orientation caused by its electric dipole moment.) This "windshield wiper effect" or "fast oscillation" is analysed in an Appendix. The amplitude was derived there to be

$$\alpha^{(F)}_{\rm max.} = 3.586\,\frac{\Delta\gamma_{\rm max}}{Q_s}. \tag{13}$$

The r.m.s. fractional energy spread is estimated to be $\sigma_{\mathcal{E}} = 0.000072$. This corresponds to $\Delta\gamma_{\max} \approx 0.00015$. From Eqs. (12) and (13),

$$\alpha^{(F)}_{\max.} = 3.586\,\frac{0.0002}{0.01} \approx 0.07. \tag{14}$$

7 Sextupole Families and SCT Compensation

- Betatron contributions to spin decoherence are proportional to $\int_0^{\mathcal{C}_0} \gamma\, ds$, where $\mathcal{C}_0$ is the ring circumference is important
- Values of these quantities for both planes are shown in bold face in Table 2.
- Since the B family of sextupoles are at maxima of β_y they can be referred to as the "vertical" sextupole family. Similarly, the A sextupoles can be referred to as the "horizontal" family. This leaves the C sextupoles for trimming the off-energy compensation.

Table 8: Strengths of SCT compensation sextupoles. Columns D and S need to be modified by factor η_D which depends on the definition of D. Since sextupole strengths and dispersion enter only in SD products, this ambiguity has little effect on sextupole compensation schemes.

family	number of units	β_x m	β_y m	D m	strength S m^{-2}
A	N^A=4	26.507	197.796	$23.583\eta_D$	S^A= $0.00465/\eta_D$
B	N^B=8	22.404	246.003	$20.972\eta_D$	S^B= $-0.00253/\eta_D$
C	N^C=4	26.482	180.192	$25.288\eta_D$	S^C= $-0.000879/\eta_D$

- The per cell compensating deflections are to be caused by sextupole families A, and B, identically-powered and situated sextupoles in each cell.
- The ring consists of eight roughly identical cells, with identical B and C sextupoles compensating on a per-cell basis.
- The C family of sextupoles provide ring-wide compensation, intended to emphasize off-energy compensation.
- Three compensation conditions have to be solved simultaneously.

Betatron compensation conditions:

$$\begin{aligned}
\frac{1}{2}\int_0^{\mathcal{C}_0}\gamma_x\,ds &= D^A N^A S^A \beta_x^A + D^B N^B S^B \beta_x^B + D^C N^C S^C \beta_x^C,\\
-\frac{1}{2}\int_0^{\mathcal{C}_0}\gamma_y\,ds &= D^A N^A S^A \beta_y^A + D^B N^B S^B \beta_y^B + D^C N^C S^C \beta_y^B. \qquad (15)
\end{aligned}$$

where N^A, N^B, and N^C, are the numbers of sextupole unit in each family. At this point we can also restore "sextupole chromatic neutrality",

$$N^A S^A {D^A}^3 + N^B S^B {D^B}^3 + N^C S^C {D^C}^3 = 0. \qquad (16)$$

For a given lattice configuration, the task then is to solve simultaneous equations for S^A, S^B, and S^C;

$$\begin{pmatrix} N^A D^A \beta_x^A & N^B D^B \beta_x^B & -N^C D^C \beta_x^C \\ N^A D^A \beta_y^A & N^B D^B \beta_y^B & -N^C D^C \beta_y^C \\ N^A {D^A}^3 & N^B {D^B}^3 & N^C {D^C}^3 \end{pmatrix} \begin{pmatrix} S^A \\ S^B \\ S^C \end{pmatrix} = \begin{pmatrix} \frac{1}{2}\int_0^{\mathcal{C}_0}\gamma_x\,ds \\ -\frac{1}{2}\int_0^{\mathcal{C}_0}\gamma_y\,ds \\ 0 \end{pmatrix}. \quad (17)$$

Copying numerical values from Section **??**, Eq. (17) becomes

$$\begin{pmatrix} 4 \times 23.583 \times 26.507 & 8 \times 20.972 \times 22.404 & -4 \times 25.288 \times 26.482 \\ 4 \times 23.583 \times 197.796 & 8 \times 20.972 \times 246.003 & -4 \times 25.288 \times 180.192 \\ 4 \times 28.583^3 & 8 \times 20.972^3 & 4 \times 25.288^3 \end{pmatrix} \begin{pmatrix} S^A \\ S^B \\ S^C \end{pmatrix} = \begin{pmatrix} 8.9/2 \\ -3.7/2 \\ 0 \end{pmatrix}. \tag{18}$$

Solving this equation yields

$$S^A = 0.004647\,\mathrm{m}^{-2} \tag{19}$$

$$S^B = -0.002534\,\mathrm{m}^{-2} \tag{20}$$

$$S^C = -0.0008787\,\mathrm{m}^{-2} \tag{21}$$

8 Further Comments on UAL/ETEAPOT

8.1 Historical

- TEAPOT was developed to show that beam would survive in the SSC at the "low" energy of 1 TeV during an injection phase lasting several minutes. The code, therefore, had to be free of spurious damping or anti-damping. i.e. it had to be *symplectic* (Hamiltonian).
- The code showed that a 4 cm bore would be sufficient.
- The requirements of proton EDM experiment are similar. One must accurately track a particle moving at (almost) the speed of light for ten minutes. This is impossible, both in practice, and in principle, using numerical integration of the differential equations.
- TEAPOT (now ETEAPOT) philosophy: "exact tracking in approximate lattice" rather than "approximate tracking in exact lattice". Certainly *exact* implies *symplectic*.
- As well as implementing electric elements, and spin tracking, UAL/ETEAPOT has to achieve this. This is approaching completion.

8.2 The Infinite Dispersion Problem

- For planar electrodes the electric field varies as $1/r$.
- The centripetal force for an orbit to be circular also varies as $1/r$.
- As a result, for "off-energy closed orbits" (which are circles) the speed/kinetic energy/momentum is independent of radius. Finite change of speed causes infinite change of radius. The dispersion is infinite.
- Even for $E \sim r^{0.2}$ there is a substantial (factor of 2.3) compression of momentum spread on entry into a bend element.
- "Emittance" is pushed from longitudinal into horizontal.

9 MAD File for the Baseline Proton EDM Ring Lattice

A MADX file, `E_pEDM-rtr1.mad`, for the baseline proton EDM lattice follows. Pathologiclly accurate parameter values are artifacts of automatic file generation. Since MAD assumes all elements to be magnetic, one cannot simply run this file in MAD. The gross survey, as well as element lengths, bend angles and inverse focal lengths for quads can be inferred from this listing, but even they have only tentative values. Also, for tuning flexibility, the lattice contains some near-zero strength elements. Tentative values for the sextupole strengths are calculated in Section **??**.

```
mbegin : marker
mend : marker
mhalf : marker
marcin : marker
mslndcent : marker
marcout : marker
strh : drift, L = 1
slndh : drift, L = 0.225
QAh : quadrupole, L = 0.15, K1 = 0.00000000066666666666666667
QBh : quadrupole, L = 0.15, K1 = -0.07886666666666667
QCh : quadrupole, L = 0.15, K1 = 0.006666666666666667
SA : sextupole, L = 0.15, K2 = -0.062/eta_D
SB : sextupole, L = 0.15, K2 = 0.03373333333333334/eta_D
SC : sextupole, L = 0.15, K2 = 0.011733333333333333/eta_D
Bh : sbend, L = 15.70796326795, ANGLE = 0.39269908169875
            ! Sectors
longsth : LINE = ( strh )
            slnd : LINE = ( slndh, &
```

```
        mslndcent, &
        slndh )
pkgA : LINE = ( QAh, &
        SA, &
        QAh )
pkgB : LINE = ( QBh, &
        SB, &
        QBh )
pkgC : LINE = ( QCh, &
        SC, &
        QCh )
Ebendh : LINE = ( Bh )
arc : LINE = ( marcin, &
        pkgC, &
        Ebendh, &
        pkgB, &
        Ebendh, &
        pkgA, &
        Ebendh, &
        pkgB, &
        Ebendh, &
        slnd, &
        Ebendh, &
        pkgB, &
        Ebendh, &
        pkgA, &
        Ebendh, &
        pkgB, &
```

```
                Ebendh, &
                pkgC, &
                marcout )
        ring : LINE = ( mbegin, &
                longsth, &
                arc, &
                longsth, &
                mhalf, &
                longsth, &
                arc, &
                longsth, &
                mend )
use, ring
```